J|A|C|S
JOURNAL OF THE AMERICAN CHEMICAL SOCIETY

COMMUNICATION

pubs.acs.org/JACS

Effect of Water on the Behavior of Semiconductor Quantum Dots in Zeolite Y: Aggregation with Framework Destruction with H−Y and Disaggregation with Framework Preservation for NH_4−Y

Hyun Sung Kim,[§] Nak Cheon Jeong,[§] and Kyung Byung Yoon*

Korea Center for Artificial Photosynthesis, Center for Microcrystal Assembly, Department of Chemistry, Sogang University, Seoul 121-742, Korea

S *Supporting Information*

ABSTRACT: Treatment of dry M^{2+}-exchanged zeolite Y (M^{2+} = Cd^{2+}, Mn^{2+}, and Zn^{2+}) with dry H_2S leads to the formation of isolated, ligand-free, subnanometer MS quantum dots (QDs) in zeolite Y with no framework destruction and with H^+ as the countercation. Treatment of the dry H^+/CdS QD-incorporating zeolites Y with dry NH_3 leads to the neutralization of H^+ to NH_4^+. During this process, the framework structure remains intact. However, small amounts of interconnected CdS QDs were formed within the zeolite Y by coalition of isolated CdS QDs at the windows. With H^+ as the countercation, isolated CdS QDs rapidly aggregate into interconnected and mesosized QDs with accompanying destruction of ~50% of sodalite cages leading to the framework rupture. With NH_4^+ as the countercation, however, the isolated QDs and zeolite framework remain intact even after exposure to the moist air for 4 weeks. Interestingly, the interconnected QDs that were formed during neutralization of H^+ with NH_3 disintegrate into isolated QDs in the air. Similar results were obtained from ZnS and MnS QDs generated in zeolite Y. Thus, ligand-free, naked, subnanometer QDs can now be safely preserved within zeolite pores under the ambient conditions for long periods of time. This finding will expedite the generation and dispersion of various QDs in zeolite pores, their physicochemical studies, and applications.

Preparation of semiconductor quantum dots (QDs) in high monodispersity, their organization into two- (2D) and three-dimensional (3D) arrays, and the stabilization of the highly unstable species in the atmosphere for long-term applications are important issues in nanoscience. Zeolites have been tested as hosts for the generation of ultrasmall (<1.5 nm) ligand-free QDs with uniform sizes, for their organization into regular arrays, and for their stabilization for extended periods of time by taking advantage of the periodically existing ultrasmall nanopores which are also uniform in size and shape.[1−27] Much have been learned during the past two decades on their generation, properties, and applications.[1−27] Surprisingly, however, the fundamental knowledge about the factors that govern the effect of adsorbed moisture on the behavior of QDs and on the host framework has not been elucidated despite the fact that most zeolites are hygroscopic, and accordingly, sorbed moisture is likely to sensitively affect the nature of the QDs, their physicochemical properties, and their applications. However, without the above knowledge, research has been done and is still being conducted on their generation, property elucidation, and application under ambient conditions simply assuming that the generated QDs will exist as intended within the zeolite pores.[1−5,18−21,23−25] Thus, to help researchers obtain meaningful results, to deepen our understanding about the behavior of QDs in zeolites, and to expedite applications of intrazeolite QDs under various conditions, the aforementioned factors were studied.

Chart 1. Structures of Zeolite Y, Its Cages, Their Geometrical Representations, and Illustration of Three Types of QDs

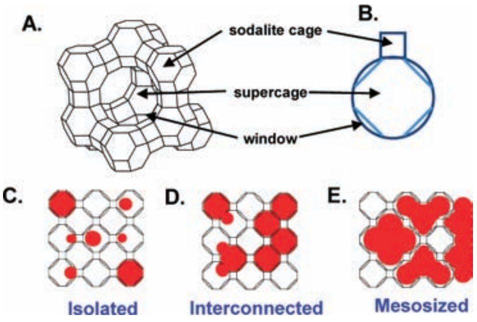

The most extensively studied zeolite is zeolite Y, and the most extensively studied QDs are CdS and the related transition metal chalcogenide QDs. In zeolite Y there are two types of cages (sodalite cage and supercage, Chart 1A and B). It has been shown that QDs exist in the supercages (Chart 1C) when they are prepared by treating metal ion exchanged zeolites with hydrogen chalcogenides in the dehydrated state.[27] For instance in the case of generation of CdS QDs in zeolite Y, the Cd^{2+}-exchanged zeolite Y is first dehydrated by evacuation at elevated temperatures (~300 °C), followed by the subsequent exposure of H_2S into the dry Cd^{2+}-exchanged zeolite Y (eq 1). This leads to the formation of not only CdS QDs but also H^+ ions within the supercages of zeolite Y. We found that the H^+ ions can be readily neutralized by adding dry ammonia gas to the CdS-incorporating zeolite Y, putting CdS QDs in an

Received: October 11, 2010
Published: January 19, 2011

Table 1. Effect of Cation and Post-Treatment on the Transformation of CdS QDs into Other Types (FW = Framework)

Cation		Dry	Moist
H^+	QD	Isolated	Interconnected + Mesosized
	FW	Intact	Destroyed
NH_4^+	QD	Isolated + Interconnected	Isolated
	FW	Intact	Intact

NH_4^+ environment (eq 2). In eqs 1 and 2, (ZO^-) denotes the negatively charged framework, and $[\ ]_{sup}$ denotes the supercage.

$$Cd^{2+}(ZO^-)_2 + H_2S \rightarrow [2H^+, CdS]_{sup}(ZO^-)_2 \qquad (1)$$

$$[2H^+, CdS]_{sup}(ZO^-)_2 + 2NH_3 \rightarrow [2NH_4^+, CdS]_{sup}(ZO^-)_2 \qquad (2)$$

The QDs in zeolite Y have been classified into '*isolated QDs*' existing in supercages (Chart 1C), '*interconnected QDs*' that are formed by interconnection of isolated QDs through the supercage windows (Chart 1D), and '*mesosized QDs*' that exist within the mesosized voids and on the external surfaces of the amorphous aluminosilicate materials that are produced by the framework rupture (Chart 1E). In the case of CdS QDs, the absorption maxima (λ_{max}) of the isolated QDs, interconnected QDs, and mesosized QDs appear in the 200−300, 300−380, and 380−480 nm regions, respectively.[27] Conversely, the absorption maxima readily serve as the probes for the identification of the nature of CdS QDs. We now report that, upon sorption of moisture, the isolated CdS QDs undergo aggregation into interconnected and mesosized QDs with accompanying framework destruction in the H^+ environment while isolated QDs and the zeolite framework remain intact in the NH_4^+ environment, and surprisingly, the interconnected CdS QDs disaggregate into isolated QDs in the NH_4^+ environment (Table 1).

The zeolite powders used in this study are nanozeolite Y with the average size of 0.1 μm and Si/Al = 1.8 having a tetramethylammonium (TMA^+) ion in each sodalite cage (denoted as $[(TMA^+)_{sod}]$-$Y_{1.8}$) and nanozeolite Y derived from $[(TMA^+)_{sod}]$-$Y_{1.8}$ by removal of TMA^+ ions by calcination (denoted as $Y_{1.8}$). For comparison, we also used commercially obtained zeolite Y powder whose Si/Al ratio is 2.5 and the average particle size is 1.0 μm (denoted as $Y_{2.5}$). While $[(TMA^+)_{sod}]$-$Y_{1.8}$ and $Y_{1.8}$ exist as individual particles; $Y_{2.5}$ exists in the aggregated state.

The diffuse reflectance UV−vis spectra of the dry, pristine CdS-encapsulated zeolite $Y_{2.5}$ with H^+ as the countercation after exposure to the moist atmosphere for 0 and 2 h, respectively (denoted as $[H^+/CdS]$-$Y_{2.5}$-0h and $[H^+/CdS]$-$Y_{2.5}$-2h, respectively), are shown in Figure 1A (Supporting Information, SI-1 and SI-2). The loaded amounts of CdS QDs in $Y_{2.5}$ were 27−29 CdS per unit cell (Supporting Information, SI-2). Indeed, while only isolated QDs exist in $[H^+/CdS]$-$Y_{2.5}$-0h (blue trace), all three types, namely, isolated, interconnected, and mesosized QDs, coexist in $[H^+/CdS]$-$Y_{2.5}$-2h (black trace). The transmission electron microscopy (TEM) image of $[H^+/CdS]$-$Y_{1.8}$-1d (Figure 1B) showed that the framework was completely destroyed and mesosized (>3 nm) QDs exist mostly on the external surface.

The diffuse reflectance spectra of the dry CdS-encapsulating zeolite Y with NH_4^+ as the countercation after exposure to the atmosphere for 0 h, 2 h, 2 d, and 4 weeks are also shown in Figure 1A (red traces). They are denoted as $[NH_4^+/CdS]$-$Y_{2.5}$-0h, $[NH_4^+/CdS]$-$Y_{2.5}$-2h, $[NH_4^+/CdS]$-$Y_{2.5}$-2d, and $[NH_4^+/CdS]$-$Y_{2.5}$-4w, respectively. As noted, small amounts of interconnected QDs were formed during the adsorption of NH_3 to dry $[H^+/CdS]$-$Y_{2.5}$ (see the shoulder band between 320 and 420 nm). Most interestingly, the interconnected CdS QDs slowly disappear with time while the absorption of the isolated QDs gradually shifts to longer wavelength regions (from 291 to 298 nm). This suggests that the disappearance of interconnected QDs occurs due to its disaggregation into isolated QDs. The simultaneous progressive red shift of the isolated QD band from 280 to 295 nm is attributed to the increase in the size of the isolated QDs by coalition of the original isolated QDs with the fragments derived from the disaggregation of the interconnected QDs. After 4 weeks, the entire interconnected band disappeared and the TEM image of $[NH_4^+/CdS]$-$Y_{1.8}$-4w showed no indication of the framework damage and the presence of mesosized CdS QDs (Figure 1C). Thus, with NH_4^+ as the countercation, the isolated CdS QDs are perfectly stable in the atmosphere and also the interconnected QDs disaggregate into isolated QDs.

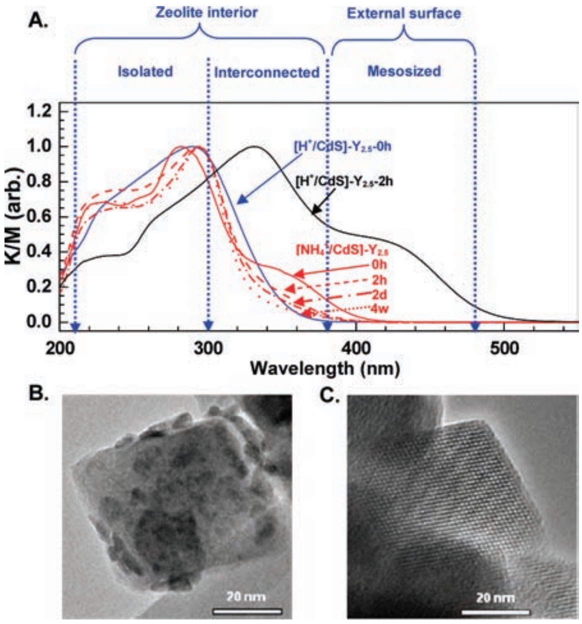

Figure 1. Diffuse reflectance spectra of various dry CdS-incorporating zeolite Y before and after exposure to the atmosphere for varying periods of time (as indicated) and the illustration of the spectral regions for isolated, interconnected, and mesosized CdS QDs (A) and TEM images of $[H^+/CdS]$-$Y_{1.8}$-1d (B) and $[NH_4^+/CdS]$-$Y_{1.8}$-4w (C).

The above results clearly show the dichotomous phenomena: in the NH_4^+ environment the ultrasmall ligand-free (isolated) CdS QDs are extremely stable in zeolite Y supercages even in the presence of sorbed water, whereas in the H^+ environment they rapidly aggregate into interconnected and mesosized QDs causing framework destruction during the aggregation. This result demonstrates for the first time that the nature of the cation or the pH of the zeolitic water (the water inside zeolite pores) is a sensitive factor that governs the effect of sorbed water on the behavior of the CdS QDs in zeolite Y.

The XRD diffraction patterns of $[H^+/CdS]$-$Y_{2.5}$, $[Na^+]$-$Y_{2.5}$, $[H^+]$-$Y_{2.5}$, and $[NH_4^+/CdS]$-$Y_{2.5}$ in their dry states and after exposure to the atmosphere for varying periods of time (Supporting Information SI-3, and Figure 2A, B, and C, respectively) show that the intensity at 2θ = 6.2° decreases by 90% with

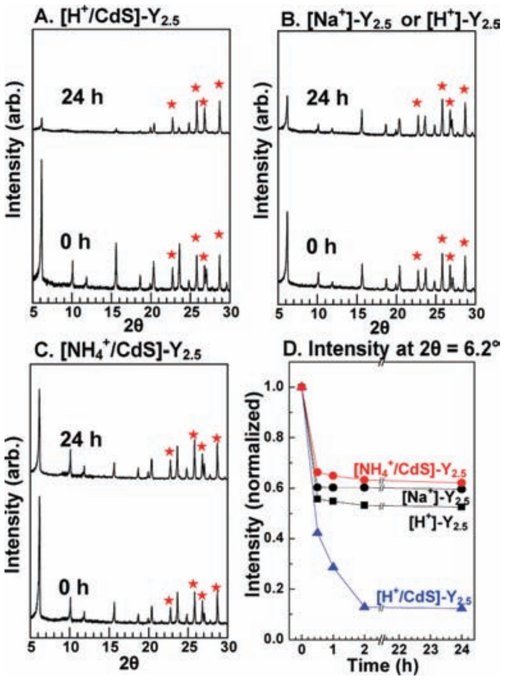

Figure 2. X-ray powder diffraction patterns of dry $[H^+/CdS]$-$Y_{2.5}$ (A), $[Na^+]$-$Y_{2.5}$ or $[H^+]$-$Y_{2.5}$ (B), and $[NH_4^+/CdS]$-$Y_{2.5}$ (C), before (bottom) and after exposure to the atmosphere for 24 h (top) and the plots of the intensity at $2\theta = 6.2°$ for each zeolite $Y_{2.5}$ (as indicated) with respect to the exposure time (D). The red star marks in A, B, and C represent the diffraction patterns of $BaSO_4$ which was added as an internal standard.

respect to the original value in the case of $[H^+/CdS]$-$Y_{2.5}$ while it decreases by 45, 40, and 38%, respectively, in the case of $[H^+]$-$Y_{2.5}$, $[Na^+]$-$Y_{2.5}$, and $[NH_4^+/CdS]$-$Y_{2.5}$, respectively, upon exposure to the atmosphere for 24 h. Figure 2D summarizes the intensity change with time. Since $[Na^+]$-$Y_{2.5}$ does not decompose regardless of the degree of hydration, the peak intensity decreases in the cases of $[H^+]$-$Y_{2.5}$, $[Na^+]$-$Y_{2.5}$, and $[NH_4^+/CdS]$-$Y_{2.5}$ are ascribed to the effect of hydration of the supercages and not to the destruction of the framework structures.[28] Therefore, the much larger decrease in peak intensity in the case of $[H^+/CdS]$-$Y_{2.5}$ is attributed to the destruction of the framework that occurs upon hydration.

To investigate the details, we also monitored the water-induced framework destruction with the magic angle spinning (MAS) solid-state NMR for ^{27}Al, ^{29}Si, and ^{13}C elements. For ^{13}C NMR study, we used $[(TMA^+)_{sod}]$-$Y_{1.8}$. To be differentiated from the TMA^+ ions existing in the sodalite cages $\{(TMA^+)_{sod}\}$, and the TMA^+ ions existing in the supercages are denoted as $(TMA^+)_{sup}$.

The ^{27}Al NMR spectra of the fully hydrated zeolite Y samples (Figure 3A) showed that small amounts of octahedrally coordinated Al appear at 0 ppm in the cases of $[H^+]$-$Y_{2.5}$ and $[H^+/CdS]$-$Y_{2.5}$. This indicates that, when hydrated, H^+ removes small amounts of Al atoms from the framework even at room temperature. Thus, hydrated H^+ gives rise to a small degree of framework destruction even at room temperature. Most interestingly, in the case of $[H^+/CdS]$-$Y_{2.5}$, even the resonances of the tetrahedrally coordinated Al atoms occur in the 10−70 ppm region, indicating that the aggregation of the isolated CdS QDs accompanies a large degree of framework destruction. It also indicates that the Al atoms in the destroyed structure adopt tetra- and pentacoordination.

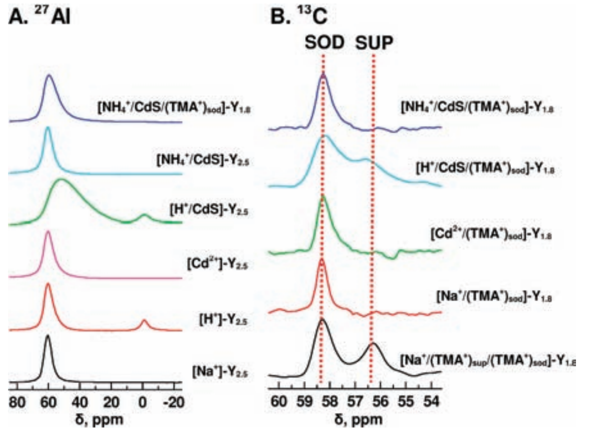

Figure 3. Magic angle spinning (MAS) solid state NMR spectra for ^{27}Al (A) and ^{13}C (B) for various zeolite Y samples (as indicated).

The ^{29}Si NMR spectra of the fully hydrated zeolite $Y_{2.5}$ samples (Supporting Information, SI-4) showed that in the case of $[H^+/CdS]$-$Y_{2.5}$ almost all of the Q4 Si atoms (the Si atoms connected to four Al atoms through the bridging O atoms) have disappeared, indicating that the Q4 site is most vulnerable to attack. This result also indicates that Al atoms next to the Q4 Si atoms are removed by H^+ ions (*vide supra*) and they get octahedrally coordinated. The ^{13}C NMR spectra of various $[(TMA^+)_{sod}]$-$Y_{1.8}$ samples (Figure 3B) show that, in the case of $[H^+/CdS/(TMA^+)_{sod}]$-$Y_{1.8}$, about 47% of the TMA^+ ions exist in the spaces larger than a sodalite cage upon hydration (Supporting Information, SI-5). This result indicates that about 47% of sodalite cages undergo large scale destruction, leading to the release of the encapsulated TMA^+ ions during water-induced aggregation of isolated CdS QDs. In contrast, the sodalite cages remain intact in $[NH_4^+/CdS/(TMA^+)_{sod}]$-$Y_{1.8}$ under the hydrated conditions even after 4 weeks.

Similar results were obtained from the nanozeolite analogues, $[H^+/CdS]$-$Y_{1.8}$ and $[H^+/CdS/(TMA^+)_{sod}]$-$Y_{1.8}$, indicating that the Si/Al ratio of the zeolite Y, particle size, and the aggregated state do not affect the nature of the produced CdS QDs and their behavior in the presence of sorbed moisture in the H^+ and NH_4^+ environments (Supporting Information, SI-6, SI-7, SI-8, and SI-9).

Thus the above results clearly show that very small isolated CdS QDs aggregate into larger QDs in zeolite in an acidic environment with accompanying framework destruction while isolated CdS QDs remain isolated and the accidently formed interconnected QDs disaggregate into isolated QDs in zeolites in a neutral or basic environment. In fact, their behavior in zeolite is a direct opposite to that of CdS in the aqueous solution since the QD particles grow bigger during their formation as pH increases (Supporting Information, SI-10). The elucidated opposite behaviors of CdS in zeolite Y and in solution indicate that the smaller QDs are more stable than larger ones in intact hydrated zeolite Y in its NH_4^+ form and that this is the driving force for the disintegration of interconnected QDs and disperses the small QDs within the pores. Similar phenomena were observed from ZnS and MnS QDs generated in zeolite Y (Supporting Information, SI-11). In the case of MnS QDs, we also found that the mesosized QDs are imbibed by zeolite Y with NH_4^+ as the countercation.

The surface coating of zeolite Y with the hydrophobic octadecyl groups was shown to be necessary to keep the isolated and interconnected QDs within the zeolite in the atmosphere when H^+ is the countercation.[26] The surface coating, however, blocks pore entrances, limiting the utilization of the isolated and interconnected QDs to only optical applications.[22] On the contrary, the isolated naked, subnanometer QDs in NH_4^+-zeolite Y have the potential to be explored for other applications such as catalysts at moderately high temperatures such as 100 °C at which the majority of the pore filling water is removed and NH_4^+ ions are stable.

This communication thus reports that the countercation sensitively affects the behavior of the metal sulfide QDs in zeolites and the stability of the zeolite framework upon hydration. We believe that this finding will expedite the elucidation of novel physicochemical properties of the ultrasmall, ligand-free semiconductor QDs in zeolites, their formation, and their applications in various fields.

ASSOCIATED CONTENT

Ⓢ Supporting Information. Detailed experimental procedure, compositions of the zeolites, and additional X-ray diffraction patterns and diffuse reflectance UV—vis spectra. This material is available free of charge via the Internet at http://pubs.acs.org.

AUTHOR INFORMATION

Corresponding Author

yoonkb@sogang.ac.kr

Author Contributions

[§]These authors contributed equally.

ACKNOWLEDGMENT

This work was supported by the Korea Center for Artificial Photosynthesis (KCAP) located in Sogang University funded by MEST through the National Research Foundation of Korea (NRF-2009-C1AAA001-2009-0093879) and Acceleration Research.

REFERENCES

(1) Wang, Y.; Herron, N. *J. Phys. Chem.* **1987**, *91*, 257–260.

(2) Herron, N.; Wang, Y; Eddy, M. M.; Stucky, G. D.; Cox, D. E.; Moller, K.; Bein, T. *J. Am. Chem. Soc.* **1989**, *111*, 530–540.

(3) Moller, K.; Eddy, M. M.; Stucky, G. D.; Herron, N.; Bein, T. *J. Am. Chem. Soc.* **1989**, *111*, 2564–2571.

(4) Stucky, G. D.; Mac Dougall, J. E. *Science* **1990**, *247*, 669–678.

(5) Liu, X.; Thomas, J. K. *Langmuir* **1989**, *5*, 58–66.

(6) Brigham, E. S.; Weisbecker, C. S.; Rudzinski, W. E.; Mallouk, T. E. *Chem. Mater.* **1996**, *8*, 2121–2127.

(7) Brühwiler, D.; Seifert, R.; Calzaferri, G. *J. Phys. Chem. B* **1999**, *103*, 6397–6399.

(8) Leiggener, C.; Calzaferri, G. *Chem.—Eur. J.* **2005**, *11*, 7191–7198.

(9) Terasaki, O.; Yamazaki, K.; Thomas, J. M.; Ohsuna, T.; Watanabe, D.; Sanders, J. V.; Barry, J. C. *Nature* **1987**, *330*, 58–60.

(10) Terasaki, O.; Yamazaki, K.; Thomas, J. M.; Ohsuna, T.; Watanabe, D.; Sanders, J. V.; Barry, J. C. *J. Solid State Chem.* **1988**, *77*, 72–83.

(11) Ozin, G. A.; Steele, M. R.; Holmes, A. J. *Chem. Mater.* **1994**, *6*, 999–1010.

(12) Jentys, A.; Grimes, R. W.; Gale, J. D.; Catlow, C. R. A. *J. Phys. Chem.* **1993**, *97*, 13535–13538.

(13) Armand, P.; Saboungi, M.-L.; Price, D. L.; Iton, L.; Cramer, C.; Grimsditch, M. *Phys. Rev. Lett.* **1997**, *79*, 2061–2064.

(14) He, J.; Ba, Y.; Ratcliffe, C. I.; Ripmeester, J. A.; Klug, D. D.; Tse, J. S.; Preston, K. F. *J. Am. Chem. Soc.* **1998**, *120*, 10697–10705.

(15) Ikeda, T.; Kodaira, T.; Izumi, F.; Ikeshoji, T.; Oikawa, K. *J. Phys. Chem. B* **2004**, *108*, 17709–17720.

(16) Sugimoto, N.; Koiwai, A.; Hyodo, S.; Hioki, T.; Noda, S. *Appl. Phys. Lett.* **1995**, *66*, 923–925.

(17) Wong, K.-L.; Souici, A.; Waele, V. D.; Mostafavi, M.; Metzger, T. H.; Mintova, S. *Langmuir* **2010**, *26*, 4459–4464.

(18) Fox, M. A.; Pettit, T. L. *Langmuir* **1989**, *5*, 1056–1061.

(19) Peng, H.; Liu, S. M.; Ma, L.; Lin, Z. J.; Wang, S. J. *J. Cryst. Growth* **2001**, *224*, 274–279.

(20) Flores-Acosta, M.; Sotelo-Lerma, M.; Arizpe-Chávez, H.; Castillón-Barraza, F. F.; Ramírez-Bon, R. *Solid State Commun.* **2003**, *128*, 407–411.

(21) Wark, M.; Sćhulz-Ekloff, G.; Jaeger, N. I. *Catal. Today* **1991**, *8*, 467–478.

(22) Kim, H. S.; Lee, M. H.; Jeong, N. C.; Lee, S. M.; Rhee, B. K.; Yoon, K. B. *J. Am. Chem. Soc.* **2006**, *128*, 15070–15071.

(23) Nath, S. S.; Chakdar, D.; Gope, G.; Kakati, J.; Kalita, B.; Talukdar, A.; Avasthi, D. K. *J. Appl. Phys.* **2009**, *105*, 094305.

(24) Bai, X.-F.; Gao, Y.; Wu, W. *Renewable Energy* **2011**, in press.

(25) Khaorapapong, N.; Ontam, A.; Ogawa, M. *Appl. Clay Sci.* **2010**, *50*, 19–24.

(26) Jeong, N. C.; Kim, H. S.; Yoon, K. B. *Langmuir* **2005**, *21*, 6038–6047.

(27) Jeong, N. C.; Kim, H. S.; Yoon, K. B. *J. Phys. Chem. C* **2007**, *111*, 10298–10312.

(28) The higher degrees in intensity decrease on going from $[NH_4^+/CdS]$-Y to $[Na^+]$-Y and to $[H^+]$-Y is ascribed to the increase in the degree of hydration due to the increase in the available pore volume.